Comparison of electrical explosions of spherical wire arrays in water and glycerol on different timescales

A. Rososhek,[1] S. Efimov,[1] S. V. Tewari,[1] D. Yanuka,[2] K. Khishchenko,[3] and Ya. E. Krasik[1]
[1]*Physics Department, Technion, Haifa 32000, Israel*
[2]*Institute of Shock Physics, Imperial College London, London SW7 2BW, United Kingdom*
[3]*Joint Institute for High Temperatures RAS, Moscow 125412, Russia*

(Received 28 February 2018; accepted 2 June 2018; published online 20 June 2018)

Results of underwater electrical explosions of spherical wire arrays in water and glycerol on the sub-microsecond timescale are presented and compared to those obtained on the microsecond timescale [Rososhek *et al.*, Phys. Plasmas **24**, 122705 (2017)]. The time-of-flight of the converging shockwave was found to be approximately the same, despite almost three times faster energy density deposition into the exploding wires for sub-microsecond timescale explosions. This phenomenon was reproduced by numerical modeling, which showed that the exploding wires' expansion on both timescales results in almost identical radii when the convergence of the shockwave becomes self-similar. Thus, to increase the shockwave convergence velocity and consequently, the parameters of the compressed water near the shockwave implosion origin, instead of increasing the energy deposition rate, one must increase the initially stored energy. *Published by AIP Publishing.*
https://doi.org/10.1063/1.5027145

I. INTRODUCTION

During the last two decades, it was demonstrated that underwater electrical explosions of single wires using moderate pulse power systems with only several kJ of stored energy can be successful for studies of Warm Dense Matter[1] (WDM) characterized by temperatures in the eV range and pressures above 10^{10} Pa.[2,3] During the explosion, a drastic increase in the wire's resistivity (up to several Ohms) occurs in the vapor → plasma phase transition accompanied by the main energy deposition and fast plasma radial expansion. The latter occurs due to the extremely high ($>10^{10}$ Pa) internal pressure inside the wire-plasma. The radial velocity of the wire expansion (up to 4×10^5 cm/s), determined by wire properties and the energy density deposition rate, exceeds the velocity of sound in water, leasing to Strong Shock Waves (SSWs). It was shown that up to 24% of the energy delivered to the wire can be transferred to water flow.[4]

For cylindrical or spherical wire arrays (SWA), the SSWs generated by each wire overlap, forming either a cylindrical or a quasi-spherical converging SSW respectively.[5] This converging SSW compresses and heats the water at the implosion origin, resulting in strong light emission during tens of nanoseconds. The time interval between the beginning of this light emission and the maximum of the discharge current (the starting point of the SSW's generation) defines the Time-Of-Flight (TOF) of the SSW. To estimate the water flow parameters, one Dimensional (1D) Hydrodynamic (HD) simulations[6] using the Equations of State (EOS) of copper,[7] water,[7] and glycerol,[8–10] were performed. The simulation assumes uniformity of the SSW convergence, includes a fitting parameter to the measured TOF, and requires that the total energy in the converging water flow is $\leq$12% of the energy delivered to the exploding wires.

Recently,[12] we studied electrical explosions using different diameters of SWA's on the microsecond (μs) timescale in water and glycerol for various energies stored in the pulse generator. It was found that the convergence of the SSW in glycerol is faster than in water resulting, according to 1D HD simulations, in several times larger pressures near the implosion origin in glycerol than in water. Also, the increase in the stored energy from 3.6 to 6.1 kJ (for fixed array diameter) or decrease in the sphere's diameter from 30 to 20 mm (for the same stored energy) leads to faster SSW implosion and, consequently, to higher pressure, temperature, and density near the implosion origin. The pressure and temperature in a spherical volume of ~0.2 mm diameter around the origin of the sphere were estimated by 1D HD simulations, which assumed uniform convergence, to be in excess of 10^{12} Pa and of several eV. Here it is understood that additional research is strongly required to confirm the SSW uniform implosion.

In this paper, we describe the results of a similar study, carried out using the sub-μs-timescale MAGEN generator[13] which allows for up to three times faster energy deposition into the exploding wires. The main objective of this research was to study the effect of the increased rate of the energy density deposition into exploding wires, for approximately the same deposited energy. We demonstrate the manifestation of self-similarity of the converging SSW, i.e., when further expansion of the exploded wires has no influence on the SSW's velocity for electrical explosions of arrays for different energies and energy density deposition rates. This issue is very important for the design of pulsed power generators with larger stored energy which can be used for the formation of dense liquid near the SSW implosion origin suitable for studies of cross-sections of light nuclei at ultra-low energies[14] as well as properties of this liquid at extreme conditions.

II. EXPERIMENTAL SETUP

The MAGEN sub-μs-timescale generator was charged to either 70 kV or 85 kV corresponding to 4.7 kJ and 6.9 kJ

stored energy, respectively. These energies are close to those used in our μs-timescale research.[12] The differential waveforms of the current and voltage were measured using B-dot and D-dot probes, respectively, placed near the load. The power was calculated as $P(t) = [\phi(t) - L(dI/dt)]I(t)$, where $\phi(t)$ is the voltage, $I(t)$ is the current, and $L = 14$ nH is the inductance of the SWA and the current path between the D-dot probe and the SWA. The error in the current and resistive voltage measurements was $\pm 5\%$. The energy deposited into the SWA was calculated as $W_d(t) = \int_0^\tau P(t)dt$, where τ is the time during which the resistive voltage drops to zero. The 20, 25, and 30 mm diameter copper SWAs were placed between the high-voltage and grounded electrodes immersed in either deionized water or glycerol. For glycerol, the SWA and the electrodes were both placed inside a Delrin box. Apart from using MAGEN, the explosion chamber (Fig. 1) and the experiments were the same as those performed in Ref. 12.

Preliminary shots showed that the discharge was almost overdamped for spherical arrays of 40 copper wires of either 114 μm or 130 μm wire diameter and for charging MAGEN with 70 kV and 85 kV, respectively. To measure the TOF of the SSW, a 1 mm optical fiber was placed in an opaque tube at the equatorial plane of the SWA.[12] One end of the fiber was attached to a Hamamatsu photomultiplier tube (PMT) connected to a Tektronix TDS-640S oscilloscope. The converging SSW's interaction with the fiber close to the implosion origin leads to intense light emission which was used for measurements of SSW TOF which was in the range 2.8–5.6 μs depending on the array radius, stored energy, and medium. As described in Ref. 12, here too, generator shots were repeated for each sphere diameter until, for two to three shots, reliable light emission from the fiber was obtained. The difference in the TOF for the same experimental conditions, but different shots of the generator, was ± 60 ns.

III. EXPERIMENTAL AND 1D HD MODELING RESULTS

Waveforms of the current, resistive voltage, power, and energy deposition for 30 mm diameter SWA explosions for charging voltages of 70 kV and 85 kV in water are shown in Fig. 2. The same results were obtained for this SWA array explosion in glycerol. One can see that the discharge is almost overdamped and that the main energy deposition into the SWA occurs during ~250 ns. Aperiodic discharges were also realized for 25 mm diameter SWA explosions in water. The difference from the μs-timescale research[12] was that for glycerol, the explosions of 25 mm diameter SWAs were characterized by fast decaying underdamped discharges, indicating the formation of a weakly ionized gas layer in the vicinity of the surface of the wires. For 20 mm diameter SWAs, fast decaying underdamped discharges for both water and glycerol were obtained similar to those described in Ref. 12. Nevertheless, even for these fast decaying discharges, the major part of the energy deposition (90%) into the exploding wires occurred during the first half of a period of the current oscillations.

The main purpose of the present study is to understand the effect of the energy deposition rate on the parameters of the SSW. Here, let us note that the energy deposited into the exploding wires depends on the discharge current rise time and was the subject of research reported in Refs. 15–17. In the present research, as well as in Ref. 12, almost overdamped electrical discharges were realized by optimizing the number of wires and wire diameters. Thus, in both studies, almost the same energy and energy density were deposited into the wire array during the time shorter than a quarter period of the underdamped discharge. Thus, the main difference between these studies is the energy deposition rate.

In Tables I and II, one can see a comparison of the electrical parameters of SWA explosions, TOF of the SSWs and the results of one-dimension (1D) hydro-dynamic (HD) simulations at $r = 10$ μm, obtained in our study with both μs-[12] and sub-μs-timescale generators. For both cases, the design of the SWAs was identical and the stored energy in the pulse generators was almost the same (within $\leq$12%). However, the energy density deposition rate into the wire array is up to three times faster when the MAGEN generator is used. The 1D HD simulations of SSW implosion were based on a model described in detail in Ref. 6 with modification described in Ref. 11, namely, a thin "Cu layer" was considered. This layer has the same total mass as the exploded wires into which electrical energy was deposited and the expansion of this layer determined the SSW velocity. The input parameter in the simulations is the energy density deposition rate into the "Cu layer," which results in a TOF of the SSW as in the experiments and the energy delivered to the liquid flow should be 12% of the energy deposited into the wires.[4] These simulations assume spherical symmetry of the SSW's convergence and used SESAME[7] Equation of States (EOS) for copper and water and the EOS for glycerol.[8–10] The SSW velocity is governed by the expansion of a Cu layer having the same mass as the Cu wires.

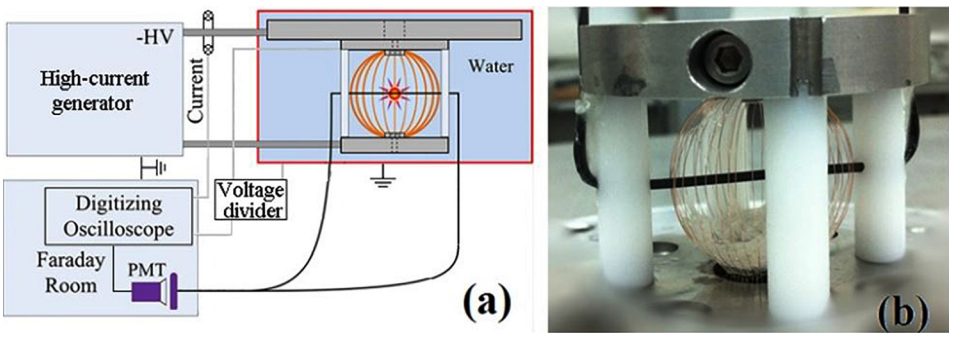

FIG. 1. Experimental setup (a) and external view of a 30 mm diameter spherical Cu wire array.

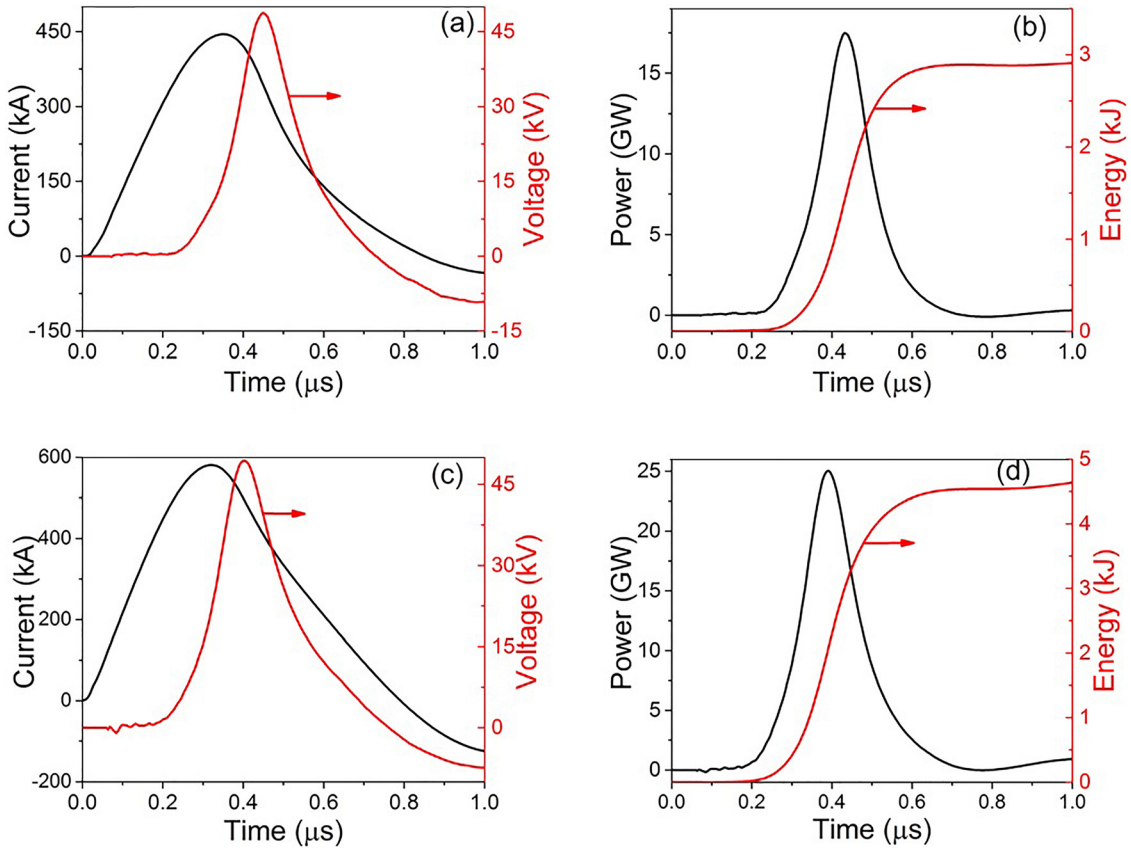

FIG. 2. Typical waveforms of the discharge current and voltage (a and c) and the power and energy deposition (b and d) for an electrical explosion of a 30 mm diameter SWA in water for charging voltages 70 kV (4.7 kJ) in (a) and (b) and 85 kV (6.9 kJ) in (c) and (d).

In Table I, one can see that the maximal resistive voltage changes only slightly between shots in water or glycerol implying that it is almost independent of the operating timescale of the pulse generator and the surrounding medium. However, because of larger current in the sub-μs-timescale explosions, the array resistance at maximal resistive voltage is twice as large for μs-timescale compared to for sub-μs-timescale explosions, for both water and glycerol. The latter can be related to the plasma formation with larger conductivity than for μs-timescale implosions. Nevertheless, the total energy deposited into the wire array due to larger current in sub-μs-timescale explosions is similar for both timescale experiments.

In Table II, one can see that similar to the results obtained in Ref. 12 for both timescales, glycerol is superior to water, that is, it provides a medium for faster SSW velocity and higher compression near the implosion origin. However, in spite of the significantly larger energy deposition rate for sub-μs-timescale implosion, the TOF of the SSW obtained for both timescale experiments is almost the same. Here, the values of the SSW TOF are the average values having a jitter of

TABLE I. Electrical parameters of SWA explosions in water and glycerol for the μs-[12] generator compared to those obtained with the sub-μs-timescale generator used in the present study.

Array dia. (mm)	Stored energy (kJ)	Medium	Maximal current (kA)	Explosion time (ns)	Maximal resistive voltage (kV)	Array resistance (mΩ)	Deposited energy (kJ)	Generator's timescale
20	4.7	Water	442	335	30.7	82	2.0	sub-μs
		Glycerol	441	335	30.5	81	2.1	
20	3.6	Water	258	840	30.0	152	2.2	μs
		Glycerol	240	810	28.0	149	2.1	
25	6.9	Water	588	330	41.8	88	4.0	sub-μs
		Glycerol	590	332	40.2	85	3.9	
25	6.1	Water	261	870	38.0	191	3.3	μs
		Glycerol	230	680	37.0	291	2.5	
30	6.9	Water	581	325	49.3	103	4.7	sub-μs
		Glycerol	589	330	44.0	99	3.9	
30	6.1	Water	310	830	45.0	198	4.9	μs
		Glycerol	317	845	44.0	213	3.6	

TABLE II. TOF of the SSW and the results of 1D HD simulations obtained at $r = 10\,\mu$m from the sphere's origin for the μs- and sub- μs-timescale[12] generators.

Array dia. (mm)	Stored energy (kJ)	Medium	TOF (ns)	Mach number	Pressure (TPa)	Density (g/cm^3)	Temperature (eV)	Generator's timescale
20	4.7	Water	3400	20.9	1.43	6.25	4.55	sub-μs
		Glycerol	2795	31.4	4.72	5.84		
20	3.6	Water	3490	20.5	1.43	6.23	4.57	μs
		Glycerol	2950	29.2	4.17	5.70		
25	6.9	Water	4340	21	1.73	6.54	5.40	sub-μs
		Glycerol	3700	31.5	4.73	5.84		
25	6.1	Water	4440	21.5	1.72	6.50	5.40	μs
		Glycerol	4030	28.4	4.07	5.70		
30	6.9	Water	5365	22.8	1.92	6.67	6.06	sub-μs
		Glycerol	4600	31.6	4.79	5.86		
30	6.1	Water	5610	21.8	1.78	6.60	5.50	μs
		Glycerol	4780	30.2	4.43	5.80		

$\pm$100 ns (Ref. 12) and $\pm$60 ns for μs- and sub- μs-timescale explosions, respectively.

In Fig. 3, the time evolution of the energy deposited into 30 mm diameter SWAs for sub-μs- and μs-timescale explosions is shown. One can see that for the sub-μs-timescale, almost the entire energy was deposited during $\sim$400 ns, while for the μs-timescale explosions, during $\sim$1300 ns. One can expect that this almost three-fold difference in the energy deposition rate, namely, $\sim 3.3 \times 10^9$ J/s and $\sim 1.1 \times 10^{10}$ J/s for μs- and sub-μs timescales, respectively, will result in considerably different flow parameters; however, as shown in Table II, the difference is negligibly small ($\sim$5%).

To explain this interesting result, let us assume a thin Cu sphere with mass equal to the mass of the spherical wire array. Electrical explosion of this sphere and its expansion can be considered as a piston generating converging SSW generation. Data shown in Fig. 3 suggest that a faster energy density deposition rate should lead to faster phase transitions and, consequently, to faster copper layer radial expansion, i.e., piston expansion. The latter should lead to larger initial velocity of the converging SSW, which in turn results in faster separation of the expanding piston and the SSW. Beginning from some distance from the piston, the SSW convergence becomes self-similar. The main question is related to the energy which the piston transfers to the SSW prior to when its convergence becomes self-similar on the different timescales and the period during which the SSW receives the energy from the piston. To answer this question, 1D HD simulations[6,11] were carried out to find the initial radius $r = r_s$ from which the SSW's convergence becomes self-similar, that is, the radius of the spherical volume in which the flow parameters and the TOF of the SSW no longer depend on the power delivered during the wire array explosion. In these simulations, the expanding piston was artificially "turned-off" by replacing it with a water layer at some time, $t = t_s$, defined as the onset time of the self-similarity. By carrying out simulations for different values of t_s, the radius r_s was found when the TOF of the SSW was the same as that obtained without artificial "turn-off" of the piston and equal to the experimentally measured TOF. The results of these simulations are presented in Table III.

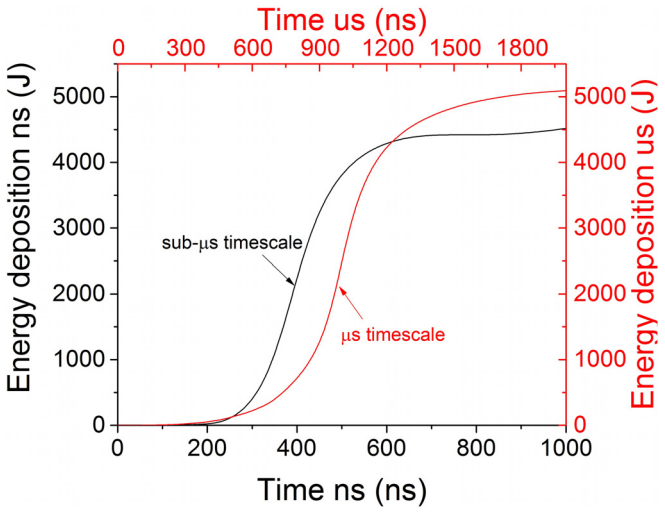

FIG. 3. Energy deposition into a 30 mm diameter SWA during an electrical explosion in water for the sub-μs-timescale (black curve and axes) and μs-timescale (red curve and axes) generators.

Here, values of t_s* and r_s and the work produced by the piston prior to t_s* and total work of the piston are presented for average values of the SSW TOF (see Table II). The errors in the values of t_s* and r_s were obtained by 1D HD simulations using the time jitter in SSW TOF, namely $\pm$100 ns (Ref. 12) and $\pm$60 ns for μs- and sub-μs-timescale explosions, respectively. These simulations showed errors in t_s* and r_s as $\pm$80 ns, $\pm$250 μm and $\pm$100 ns, and $\pm$300 μm for μs- and sub-μs-timescale explosions, respectively. The same simulations showed that the errors in piston work, as a result of time jitter in TOF, were $\pm$15 J for μs-timescale and $\pm$30 J for sub-μs-timescale explosions.

As expected, on the sub-μs-timescale, the initial velocity of the piston and, consequently, the initial SSW velocity are larger than on the μs-timescale explosions. However, the time interval during which the piston transfers its energy to the SSW is shorter. One can see that by the time the SSW reaches self-similarity, on both timescales, it also approaches almost the same radius for explosions of SWAs of equal radii. In addition, comparing explosions in water on different timescales of arrays with the same radius, one can see that the energy delivered to the water flow by the piston prior to

TABLE III. Results of 1D HD simulations[6,11] used to investigate the self-similarity of the converging SSW.

Medium	Array diam. (mm)	Time-scale	t_s*[a] (ns)	r_s (mm)	Work done by the piston prior to t_s*[b] (J)	Total work of the piston (J)
Water	20	sub-μs	760	8.80	252	332
water	20	μs	1410	8.60	286	406
Water	25	sub-μs	8450	11.10	420	543
Water	25	μs	1450	11.10	439	485
Water	30	sub-μs	950	13.30	626	774
Water	30	μs	1580	13.40	602	650
Glycerol	20	sub-μs	680	8.90	238	329
Glycerol	20	μs	1210	8.90	150	223
Glycerol	25	sub-μs	700	11.40	308	441
Glycerol	25	μs	1220	11.30	171	278
Glycerol	30	sub-μs	790	13.70	418	566
Glycerol	30	μs	1340	13.70	275	412

[a]t_s* is defined relative to the beginning of the discharge current.
[b]Part of the total work of the piston is the ratio between the "work produced by the piston" before the self-similar SSW convergence starts to the total work produced by the piston during its expansion.

when the SSW's convergence becomes self-similar is almost the same. The latter explains the same flow parameters formed by these SSWs near the implosion origin.

This equality of the energy delivered to the water flow by the piston prior to when the SSW's convergence becomes self-similar on different timescales of array explosions does not hold for explosions in glycerol. One can see in Table III that this energy is ~1.6 times larger for sub-μs than for μs-timescale array explosions, for almost the same values of r_s. However, the data presented in Table II show approximately the same SSW velocities near the implosion origin for both timescales. To explain this apparent contradiction, one should account for the glycerol's partial combustion for the longer μs-timescale explosions which delivers additional energy to the converging SSW.

These data raise the following question: what affects the TOF of the converging SSW more, the energy deposition rate (here the operating "timescale" of the pulse power generator), or the amount of energy stored in the generator. To answer this question, we carried out additional 1D HD simulations for the same energy (6 kJ) stored in the μs-timescale generator, but with ten-fold faster current rise time. These simulations produced the same TOF of the SSW (within 5% of the values obtained on our μs-timescale generator). Here, the time when the SSW starts its self-similar convergence is much shorter due to the larger initial velocity of the piston's expansion, i.e., the SSW rapidly accumulates sufficient energy when it approaches r_s, but the TOF remains the same. Thus, one can conclude that the total energy stored in the pulse generator has a dominant impact on the velocity of the SSW and, consequently, on the extreme parameters of the medium near the implosion origin.

IV. CONCLUSION

The results obtained in experiments with underwater electrical explosions of SWAs on the sub-μs- and μs-timescales with high-current generators resulted in identical TOFs of the SSWs and, consequently, the same flow parameters near the implosion origin for sub-μs- and μs-timescale experiments for approximately the same stored energies in the generators and the same array diameters and background environment despite an almost three times larger energy deposition rate for sub-μs-timescales. This self-similarity, for the timescales studied here, appears because the energy transferred to the water flow while the SSW approaches r_s is independent of the rate of the energy deposition into the wires. Using 1D HD simulations, it was shown that the self-similar convergence of the SSW starts earlier for the sub-μs timescale array explosions, but the initial self-similar radius of the SSW was found to be almost the same for both timescale experiments. The latter is explained by a shorter time interval of the energy transfer to the medium by the expanding piston for sub-μs-explosions. Thus, in order to increase the SSW implosion velocity, and, consequently, to increase pressure, density, and temperature of the medium near the SSW implosion origin, increasing the initially stored energy of a μs-timescale pulsed generators (simpler than sub-μs-timescale generators) is sufficient. In addition, the results obtained for sub-μs-timescales confirmed the data obtained in Ref. 12, namely, the electrical explosion of SWAs in glycerol results in faster converging SSWs than in water for the same amount of initially stored energy and the same array diameter.

ACKNOWLEDGMENTS

We thank Dr. J. Leopold for critical reading and helpful comments. This research was supported by the Center for Absorption in Science, Ministry of Immigrant Absorption, State of Israel. S. V. Tewari would like to thank Science and Engineering Research Board, India, for the award of Overseas Postdoctoral Fellowship.

[1]V. E. Fortov and I. T. Iakubov, *The Physics of Non-Ideal Plasma* (World Scientific, Singapore, 2000).
[2]A. W. DeSilva and J. D. Katsouros, Phys. Rev. E **57**, 5945 (1998).
[3]Ya. E. Krasik, A. Grinenko, A. Sayapin, S. Efimov, A. Fedotov, V. Tz. Gurovich, and V. I. Oreshkin, IEEE Trans. Plasma Sci. **36**, 423 (2008), and references therein.
[4]S. Efimov, V. T. Gurovich, G. Bazalitski, A. Fedotov, and Y. E. Krasik, J. Appl. Phys. **106**, 073308 (2009).
[5]Y. E. Krasik, S. Efimov, D. Sheftman, A. Fedotov-Gefen, O. Antonov, D. Shafer, D. Yanuka, M. Nitishinskiy, M. Kozlov, L. Gilburd, G. Toker, S. Gleizer, E. Zvulun, V. Tz. Gurovich, D. Varentsov, and M. Rodionova, IEEE Trans. Plasma Sci. **44**, 412 (2016), and references therein.
[6]G. Bazalitski, V. T. Gurovich, A. Fedotov-Gefen, S. Efimov, and Y. E. Krasik, Int. J. Shock Waves, Detonations Explos. **21**, 321 (2011).
[7]*SESAME: The Los Alamos National Laboratory Equation-of-State Database*, edited by S. P. Lyon and J. D. Johnson, Los Alamos National Laboratory, Report No. LA-UR-92–3407, 1992.
[8]I. V. Lomonosov, V. E. Fortov, and K. V. Khishchenko, Khim. Fiz. **14**, 47–52 (1995).
[9]A. V. Bushman, M. V. Zhernokletov, I. V. Lomonosov, V. E. Fortov, K. V. Khishchenko, and Y. N. Sutulov, J. Exp. Theor. Phys. **82**, 895–899 (1996).
[10]K. V. Khishchenko, I. V. Lomonosov, and V. E. Fortov, AIP Conf. Proc. **370**, 125–128 (1996).
[11]L. Gilburd, S. Efimov, A. F. Gefen, V. T. Gurevich, G. Bazalitski, O. Antonov, and Y. E. Krasik, Laser Part. Beams **30**, 215 (2012).
[12]A. Rososhek, S. Efimov, M. Nitishinski, D. Yanuka, S. V. Tewari, V. T. Gurovich, K. Khishchenko, and Y. E. Krasik, Phys. Plasmas **24**, 122705 (2017).
[13]B. M. Kovalchuk, A. V. Kharlov, V. B. Zorin, and A. A. Zherlitsyn, Rev. Sci. Instrum. **80**, 083504 (2009).

[14]V. M. Bystritsky, V. M. Grebenyuk, S. S. Parzhitski, F. M. Penkov, V. T. Sidorov, V. A. Stolupin, T. L. Bulgakov, G. A. Mesyats, A. A. Sinebryukhov, V. A. Sinebryukhov, S. A. Chaikovsky, A. V. Luchinsky, V. I. Makhrin, N. A. Ratakhin, S. A. Sorokin, V. M. Bystriskii, M. Filipowitcz, J. Wozniak, and E. Gula, Laser Part. Beams **18**, 325 (2000), and references therein.

[15]A. G. Rousskikh, V. I. Oreshkin, A. Y. Labetsky, S. A. Chaikovsky, and A. V. Shishlov, Tech. Phys. **52**, 571 (2007).

[16]A. G. Rousskikh, R. B. Baksht, V. I. Oreshkin, and A. V. Shishlov, AIP Conf. Proc. **651**, 217 (2002).

[17]A. Virozub, V. T. Gurovich, D. Yanuka, O. Antonov, and Y. E. Krasik, Phys. Plasmas **23**, 092708 (2016).